Environmental Research 242 (2024) 117623

Contents lists available at ScienceDirect

Environmental Research

journal homepage: www.elsevier.com/locate/envres

Microcystin profiles in European noble crayfish *Astacus astacus* and water in Lake Steinsfjorden, Norway

Christopher O. Miles [a,b], David A. Strand [a], Johannes C. Rusch [a], Andreas Ballot [c], Sigrid Haande [c], Kjersti L.E. Løvberg [a], Trude Vrålstad [a], Ingunn A. Samdal [a,*]

[a] Norwegian Veterinary Institute, Elizabeth Stephansens vei 1, 1433, Ås, Norway
[b] National Research Council Canada, Halifax, Nova Scotia, B3H 3Z1, Canada
[c] Norwegian Institute for Water Research, Økernveien 94, 0579, Oslo, Norway

ARTICLE INFO

Keywords:
Cyanobacteria
ELISA
Food safety
LC–HRMS
Microcystins
Planktothrix

ABSTRACT

Lake Steinsfjorden, an important noble crayfish (*Astacus astacus*) habitat, is often affected by blooms of *Planktothrix* spp. that produce microcystins (MCs). A poor correlation between MCs by ELISA in the water and in crayfish tissue in a study in 2015 prompted further investigation by LC–HRMS. LC–HRMS analyses of filters from water samples and on selected crayfish tissue extracts from the 2015 study revealed the presence of known and previously unreported MCs. Crayfish samples from May and June 2015 were dominated by MCs from the *Planktothrix* bloom, whereas in September novel MCs that appeared to be metabolites of MC-LR were dominant, even though neither these nor MC-LR were detected in the water in 2015. A water sample from October 2016 also showed MCs typical of *Planktothrix* (i.e., [D-Asp^3]- and [D-Asp^3,Dhb^7]MC-RR and -LR), but low levels of MC-RR and MC-LR were detected in the lake water for the first time. In late summer and autumn, the MC profiles of crayfish were dominated by the homonorvaline (Hnv) variant MC-LHnv, a putative metabolite of MC-LR. Taken together, ELISA, LC–HRMS and previous PCR analyses showed that although *Planktothrix* was part of the crayfish diet, it was not the sole source of MCs in the crayfish. Possibly, crayfish in Lake Steinsfjorden may be ingesting MCs from benthic cyanobacteria or from contaminated prey. Therefore, information on the cyanobacterial or MC content in the water column cannot safely be used to make predictions about MC concentrations in the crayfish in Lake Steinsfjorden. Interestingly, the results also show that targeted LC–MS analysis of the crayfish would at times have underestimated their MC content by nearly an order of magnitude, even if all previously reported MC variants had been included in the analysis.

1. Introduction

The noble crayfish (*Astacus astacus*) is a valued delicacy for human consumption, and Lake Steinsfjorden is one of the most important locations for harvesting crayfish in Norway (Skurdal et al., 2002). Although this native European crayfish species is classified as "vulnerable" on the IUCN red list (IUCN, 2022), and "endangered" on the Norwegian red list (Artsdatabanken, 2021), it is also of great cultural and economic significance and therefore protection is a priority in Norway. Thus, the Norwegian legislation and management of noble crayfish allows for a strictly regulated fishery (Johnsen and Vrålstad, 2017). The noble crayfish population in Lake Steinsfjorden has been stable for the last 10 years (Johnsen et al., 2019) and accounts for approximately 25–30% of the annual harvest in Norway (Johnsen et al., 2019; Skurdal et al., 2002).

Lake Steinsfjorden is a dimictic and mesotrophic lake with a maximum depth of 24 m and a surface area of 13.9 km^2, which is located in southeastern Norway (Halstvedt et al., 2007). The larger and deeper

Abbreviations: Adda, 3*S*-amino-9*S*-methoxy-2*S*,6,8*S*-trimethyl-10-phenyl-4*E*,6*E*-decadienoic acid; AGC, automatic gain control; CE, collision energy; DDA, data-dependent acquisition; Dha, dehydroalanine; Dhb, dehydrobutyrine; DIA, data-independent acquisition; DMAdda, 9-*O*-demthylAdda; DMSO, dimethyl sulfoxide; ELISA, enzyme-linked immunosorbent assay; Hnv, 5-hydroxynorvaline; LC–HRMS, liquid chromatography–high-resolution mass spectrometry; LoD, limit of detection; maxIT, maximum injection time; MC, microcystin; Mdha, *N*-methyldehydroalanine; Mlan, *N*-methyllanthionine; Mser, *N*-methylserine; Nao, N^5-acetyl-ornithine; RDBE, rings plus double-bond equivalents; SD, standard deviation.

* Corresponding author.
E-mail address: ingunn.samdal@vetinst.no (I.A. Samdal).

https://doi.org/10.1016/j.envres.2023.117623
Received 24 August 2023; Received in revised form 18 October 2023; Accepted 7 November 2023
Available online 11 November 2023
0013-9351/© 2023 The Authors. Published by Elsevier Inc. This is an open access article under the CC BY license (http://creativecommons.org/licenses/by/4.0/).

Lake Tyrifjorden is connected to the southern end of Lake Steinsfjorden through a narrow shallow passage with a low water exchange (Halstvedt et al., 2007). Lake Steinsfjorden is popular for recreational activities such as swimming, fishing and water sports, and water from the lake is also used for irrigation of nearby farmland.

Cyanobacterial blooms of *Planktothrix agardhii* and *Planktothrix rubescens* occur frequently in Lake Steinsfjorden (Halstvedt et al., 2007; Rohrlack et al., 2008), and both are known to produce cyanotoxins such as the microcystins (MCs). *Planktothrix* spp. can form metalimnetic blooms at 10−12 m depth during their growth season in Lake Steinsfjorden (Halstvedt et al., 2007). *Planktothrix* filaments become evenly distributed throughout the whole waterbody of the lake by the autumnal circulation, where they can survive in large quantities under the ice cover during winter. These filaments are released in the spring thaw, accumulating both in shallow areas and on the shore (Samdal et al., 2020). Consumption of *Planktothrix* filaments by the omnivorous crayfish in Lake Steinsfjorden was demonstrated by PCR analysis (Samdal et al., 2020), confirming this as a potential route of exposure to cyanobacterial toxins, including MCs.

MCs are toxic cyclic heptapeptides, with the unusual β-amino acid 3*S*-amino-9*S*-methoxy-2*S*,6,8*S*-trimethyl-10-phenyl-4*E*,6*E*-decadienoic acid (Adda) at position-5 (Fig. 1). So far, around 300 MC analogues have been identified, with the most commonly reported MCs being MC-RR (**5**), MC-YR, MC-LR (**12**), and MC-LA (**27**) (Bouaïcha et al., 2019; Jones et al., 2021). Although none of these four variants have been found in Lake Steinsfjorden, a series of MCs have been recorded in the lake or from *Planktothrix* cultures isolated from the lake. In earlier studies these were reported as desmethylMC-LR, desmethylMC-RR, desmethylMC-HtyR, and desmethylMC-YR (Rohrlack et al., 2008) due to the difficulty of identifying the position of the demethylation by LC–MS/MS. Two later papers reported [D-Asp^3,Dhb^7]MC-RR (**4**), [D-Asp^3]MC-RY, and [D-Asp^3]MC-LY, as well as analogues tentatively identified as [D-Asp^3]MC-RR (**3**), [D-Asp^3,DMAdda^5,Dhb^7]MC-LR, [D-Asp^3,Dhb^7]MC-LR (**9**), [D-Asp^3,Dhb^7]MC-HtyR (**8**), [D-Asp^3]MC-HtyR, [D-Asp^3]MC-LR (**10**), [D-Asp^3,Dhb^7]MC-RY, and [D-Asp^3,Dhb^7]MC-LY, together with low levels of several other analogues in water samples or *Planktothrix* cultures obtained from Lake Steinsfjorden (Mallia et al., 2019; Miles et al., 2013a).

Decapods, including freshwater crabs, crayfish and shrimps, are known to accumulate MCs in various organs, especially the hepatopancreas and gonads (Bownik, 2013; Lirås et al., 1998; Tricarico et al., 2008). In general, MC levels in contaminated decapods are highest in the hepatopancreas, stomach, and intestine, and lowest in the (tail) muscle (Gutierrez-Praena et al., 2013; Papadimitriou et al., 2012; Samdal et al., 2020; Tricarico et al., 2008). Mortalities of white shrimp have been reported in aquaculture ponds during blooms of *Microcystis aeruginosa* and an *Anabaena* sp., where up to 55 μg/g MC-LR had accumulated in the hepatopancreas, but MC-LR concentrations were below 0.1 μg/g in the tail muscle (Bownik, 2013). MCs were found to accumulate in the hepatopancreas of North American signal crayfish (*Pacifastacus leniusculus*) fed on toxic and nontoxic *Planktothrix agardhii* for two weeks, without any detectable negative effects on their health (Lirås et al., 1998), and a few studies have also examined the accumulation of MCs in the noble crayfish (Gutierrez-Praena et al., 2013; Miles et al., 2013a; Papadimitriou et al., 2012). A report from 1997 (Aune et al., 1997) proposed that noble crayfish in Lake Steinsfjorden might accumulate MCs. This was later confirmed by (Miles et al., 2013a), highlighting the need for a more comprehensive study with modern analytical tools.

A recent field study by Samdal et al. (2020) investigated the uptake and distribution of MCs in crayfish in Lake Steinsfjorden in 2015, and discovered a good correlation between *Planktothrix* cell counts and MC levels (by Adda-ELISA) in the lake water. However, MC levels in the crayfish tissues by multihapten MC-ELISA showed no correlation with *Planktothrix* or MCs by Adda-ELISA in the water in 2015 (Fig. S5 of Samdal et al. (2020)), nor in 2016 (Samdal et al., 2020). The authors suggested that this might be due either to very slow depuration of the MCs in the crayfish from the previous year or to alternative uptake routes through bioaccumulation from the food web. However, the information on the concentration of total MCs present in the samples was only obtained through ELISAs. Without information on the toxin profiles in the water and crayfish, no further conclusions were drawn, apart from that the MC content in the crayfish in Lake Steinsfjorden cannot be predicted from the MC content of the water in the lake.

During the study from 2014 to 16, Lake Steinsfjorden contained relatively high *Planktothrix* biomasses (up to 2.0 mg/L in the epilimnion (0–7 m) and 4.7 mg/L in the metalimnion (8–14 m) (Fig. 2)) at the sampling station, when compared to previous and subsequent years (Fig. S1 in Samdal et al. (2020)). *Planktothrix* spp. dominated in the lake from May–July 2015, but diatoms (*Bacillariophyceae*) were the dominant algae from August–October. *Planktothrix* spp. survived under the ice during the winter of 2014–15 and large piles of *Planktothrix* biomass were observed when the ice broke up in spring.

The aim of this study was to investigate the MC profiles by LC–HRMS in the same set of extracts of crayfish tissues (stomach, intestine, hepatopancreas and tail muscle) from 2015 to 2016 that were used for the original ELISA analysis of Samdal et al. (2020), and to compare these with the MC profile from the water in Lake Steinsfjorden during May–September 2015 and with a water sample from October 2016. It was anticipated that this might reveal details of the uptake, metabolism, and depuration of MCs in *A. astacus*, which were inaccessible in the previous study because the immunoassay methods used by Samdal et al. (2020) revealed only the total concentrations of MCs in the samples.

2. Materials and methods

2.1. Materials

Inorganic chemicals and organic solvents were reagent grade or better. The standard of MC-LR for the multihapten-ELISA was obtained from Enzo Life Sciences Inc. (Farmingdale, NY, USA), and was calibrated in-house against CRM-MC-LR from NRC (Halifax, NS, Canada). The standard for the Adda-ELISA was as provided with the kit (Abraxis LLC, Warminister, PA, USA). A mixed standard of MC CRMs prepared from CRM-MCRR (**5**), CRM-MCLR (**12**), CRM-dmMCLR (**11**), CRM-Leu^{1}MCLY, and CRM-NODR (all from NRC, Halifax, NS, Canada) was used for LC–HRMS quantitation. Mixtures of retention-time standards were prepared from [D-Asp^3]MC-RR (**3**), [D-Asp^3,Dhb^7]MC-RR (**4**), [D-Asp^3]MC-LR (**10**), MC-LA (**27**), MC-LY (**28**), MC-LW (**31**), MC-LF (**33**), MC-YR, MC-HilR, and MC-WR sourced from Abraxis, and from MC-RY purified from a bloom material (Miles et al., 2013b). In addition, extracts of cultures or field samples containing a wide range of MCs identified in previous studies were used (Ballot et al., 2020; Mallia et al., 2019; Miles et al., 2013b), together with an in-house reference material (Hollingdale et al., 2015), as qualitative standards and for comparison of LC–MS/MS spectra with those of MCs in the crayfish and water samples.

2.2. Water filter samples

Samples were taken monthly from May to October in 2015 at 1 m intervals (0–14 m) at the deepest part of the lake (60.09452 °N, 10.32427 °E), by filtering 100 mL of lake water through a cellulose nitrate membrane filter (0.45 μm, diameter 40 mm; Sartorius AG, Göttingen, Germany). The filters were dried at ambient temperature overnight and stored at −20 °C in the dark until used. All the filters from each sampling date were cut into 3 strips and placed together in a glass scintillation vial, and MeOH–water (1:1, 15 mL) was added. The vials were briefly bath-sonicated (1 min), then vortex-mixed (500 Hz for 1 h at 25 °C; Multitherm mixer, Benchmark Scientific, Edison, NJ, USA). Aliquots (1 mL) of the methanolic extracts were filtered (0.22 μm; Corning Costar Spin-X centrifuge tube filters, Sigma–Aldrich, St. Louis, MO, USA) for analysis by LC–HRMS.

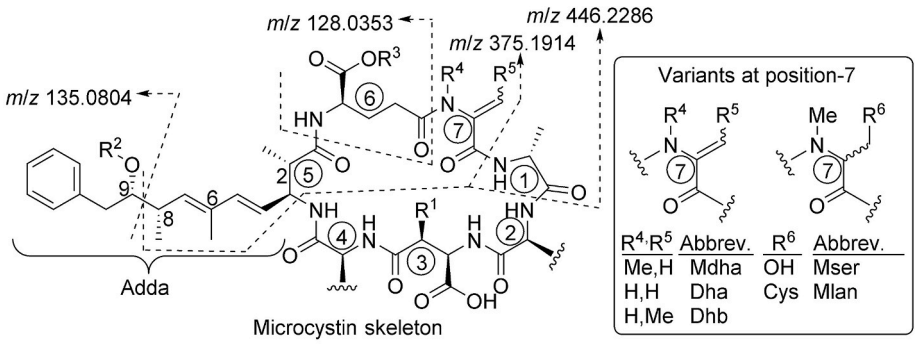

		②	④	⑦	R^1	R^2	R^3	$[M-H]^-$ *m/z*	+z	$[M+H]^+$ *m/z*
1	[D-Asp^3,Mlan^7]MC-RR	Arg	Arg	Mlan	H	Me	H	1143.5626	2	573.2922
2	[D-Asp^3,Mlan^7]MC-RR	Arg	Arg	Mlan	H	Me	H	1143.5626	2	573.2922
3	[D-Asp^3]MC-RR	Arg	Arg	Mdha	H	Me	H	1022.5429	2	512.7824
4	[D-Asp^3,Dhb^7]MC-RR	Arg	Arg	Dhb	H	Me	H	1022.5429	2	512.7824
5	MC-RR	Arg	Arg	Mdha	Me	Me	H	1036.5585	2	519.7902
6	[DMAdda^5]MC-LR	Leu	Arg	Mdha	Me	H	H	979.5258	1	981.5404
7	[Mlan^7]MC-LR	Leu	Arg	Mlan	Me	Me	H	1114.5612	2	558.7915
8	[D-Asp^3,Dhb^7]MC-HtyR	Hty	Arg	Dhb	H	Me	H	1043.5208	1	1045.5353
9	[D-Asp^3,Dhb^7]MC-LR	Leu	Arg	Dhb	H	Me	H	979.5258	1	981.5404
10	[D-Asp^3]MC-LR	Leu	Arg	Mdha	H	Me	H	979.5258	1	981.5404
11	[Dha^7]MC-LR	Leu	Arg	Dha	Me	Me	H	979.5258	1	981.5404
12	MC-LR	Leu	Arg	Mdha	Me	Me	H	993.5415	1	995.5560
13	[Mlan^7]MC-LHnv	Leu	Hnv	Mlan	Me	Me	H	1073.5235	1	1075.5380
14	[Mlan^7]MC-LHnv	Leu	Hnv	Mlan	Me	Me	H	1073.5235	1	1075.5380
15	[DMAdda^5]MC-LHnv	Leu	Hnv	Mdha	Me	H	H	938.4881	1	940.5026
16	MC-LCit	Leu	Cit	Mdha	Me	Me	H	994.5255	1	996.5401
17	[D-Asp^3]MC-LHnv	Leu	Hnv	Mdha	H	Me	H	938.4881	1	940.5026
18	[Mser^7]MC-LHnv	Leu	Hnv	Mser	Me	Me	H	970.5143	1	972.5288
19	dmMC-LHnv	Leu	Hnv	Mdha	Me	Me	H	938.4881	1	940.5026
20	MC-LM(O)	Leu	Met(O)	Mdha	Me	Me	H	984.4758	1	986.4903
21	[Dha^7]MC-LHnv	Leu	Hnv	Dha	Me	Me	H	938.4881	1	940.5026
22	MC-LNao	Leu	Nao	Mdha	Me	Me	H	993.5303	1	995.5448
23	[Glu(OMe)^6]MC-LHnv	Leu	Hnv	Mdha	Me	Me	Me	966.5194	1	968.5339
24	dmMC-LHnv	Leu	Hnv	Mdha	Me	Me	H	938.4881	1	940.5026
25	MC-LHnv	Leu	Hnv	Mdha	Me	Me	H	952.5037	1	954.5183
26	MC-HilHnv	Hil	Hnv	Mdha	Me	Me	H	966.5194	1	968.5339
27	MC-LA	Leu	Ala	Mdha	Me	Me	H	908.4775	1	910.4920
28	MC-LY	Leu	Tyr	Mdha	Me	Me	H	1000.5037	1	1002.5183
29	MC-LAbu	Leu	Abu	Mdha	Me	Me	H	922.4931	1	924.5077
30	MC-LM	Leu	Met	Mdha	Me	Me	H	968.4809	1	970.4954
31	MC-LW	Leu	Trp	Mdha	Me	Me	H	1023.5197	1	1025.5342
32	MC-LV	Leu	Val	Mdha	Me	Me	H	936.5088	1	938.5233
33	MC-LF	Leu	Phe	Mdha	Me	Me	H	984.5088	1	986.5233
34	MC-LL	Leu	Leu	Mdha	Me	Me	H	950.5244	1	952.5390
35	isoMC-LL	Leu	Leu	Mdha	Me	Me	H	950.5244	1	952.5390
36	[Dha^7]MC-RR	Arg	Arg	Dha	Me	Me	H	1022.5429	2	512.7824
37	[D-Asp^3]MC-HtyR	Hty	Arg	Mdha	H	Me	H	1043.5208	1	1045.5353
38	[Dha^7]MC-HtyR	Hty	Arg	Dha	Me	Me	H	1043.5208	1	1045.5353

Fig. 1. Structures of MCs identified in the samples, and showing characteristic positive and negative mode fragments for MC-LR (**12**). Compound numbers in the text, Figures and Tables refer to the MC variants listed here. Compounds **13**–**26** and **35** do not appear to have been reported previously, and their tentative identities are based only on LC–HRMS/MS and chemical reactivity data. The positions of demethylation for some dmMC-LHnv variants could not be determined from the available data. Compounds **36**–**38** were only detected indirectly by mercaptoethanol derivatization, due to chromatographic overlap of the underivatized compounds with major isomer(s). An additional partly characterized variant with $[M+H]^+$ at *m/z* 972.5288 (**25** + H_2O) was also detected at 10.92 min (Table S3).

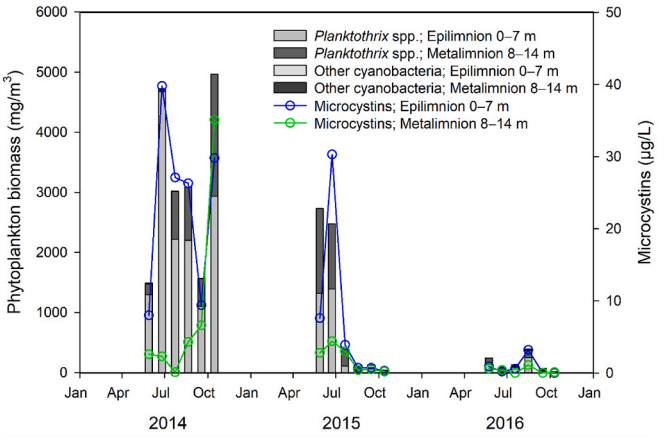

Fig. 2. Cyanobacterial biomass and MC concentrations by Adda-ELISA in Lake Steinsfjorden for 2014–2016 at respectively 0–7 m and 8–14 m. Note that "Other cyanobacteria" were present at all times, but concentrations never exceeded 36 mg/m^3. For further details, such as other phytoplankton, see also Fig. 3 in Samdal et al. (2020).

2.3. Water samples

Monthly integrated water samples for phytoplankton composition and biomass and for MC analyses were taken from May–October in 2014, 2015 and 2016 at the deepest part of the lake (STL) (Fig. 1 of Samdal et al. (2020)). A Ramberg sampler (2-m) was used to collect samples from 0 to 7 m and 8–14 m.

For quantitative phytoplankton analysis, a 100 mL subsample was removed from a sample taken from the integrated samples and preserved with Lugol's solution and a concentrated net sample (mesh size 20 µm) was taken and preserved by addition of formaldehyde (4% final concentration) for qualitative analysis. A 5 mL subsample was taken and stored at −20 °C for further analysis of total MCs by Adda-ELISA.

2.4. Phytoplankton

Phytoplankton taxa were counted and determined as described by Samdal et al. (2020). The water samples collected from Lake Steinsfjorden were tested for MCs using the MC-Adda ELISA (Abraxis LLC, Warminister, PA, USA) as described in Samdal et al. (2020). The test is an indirect competitive ELISA based on the recognition by specific antibodies of the Adda moiety found in most MCs and nodularins.

2.5. European noble crayfish (Astacus astacus)

Wild crayfish were caught using baited traps once a month from June to October 2015 by a local landowner with permission from the county governor of Buskerud as described by Samdal et al. (2020). Twenty crayfish per month (total of 100; 42 female, 58 male) with an average length of 91 mm (SD 6.5 mm) were thus analysed from 2015, and a total of 10 crayfish (4 female, 6 male) were analysed from October 2016. The crayfish were dissected in a partly-thawed condition, using clean equipment for each crayfish. Tissue samples were taken from the stomach, hepatopancreas, intestine and abdominal tail muscle and extracted as described by Samdal et al. (2020). The concentration of MCs in each crayfish extract was determined by indirect competitive ELISA as described by Samdal et al. (2020), based on the multihapten approach (Samdal et al. (2014)) with only minor adjustments to plate-coater and antibody concentrations to optimize the assay.

2.6. LC–HRMS analysis

The method, based on Yilmaz et al. (2019) and Foss et al. (2018), used a Q Exactive HF Orbitrap mass spectrometer equipped with a heated electrospray ionization interface (ThermoFisher Scientific, Waltham, MA, USA) using an Agilent 1200 G1312B binary pump, G1367C autosampler and G1316B column oven (Agilent, Santa Clara, CA, USA) connected to a Symmetry C18 column (3.5 µm, 150 × 2.1 mm; Waters, Milford, MA, USA) held at 40 °C. Analyses were performed with mobile phases A and B of H_2O and CH_3CN, respectively, each of which contained formic acid (0.1% v/v). Gradient elution (0.3 mL/min) was from 20 to 90% B over 18 min, then to 100% B over 0.1 min and a hold at 100% B (2.9 min), then returned to 20% B over 0.1 min with a hold at 20% B (3.9 min) to equilibrate the column (total run time 25 min). Injection volume was typically 1–5 µL. Extraction of product-ion masses, and the inclusion and exclusion lists for data-dependent acquisition (DDA), were performed with the mass tolerance set to 5 ppm.

The MS was operated in positive ion mode and calibrated from *m/z* 74–1922. The spray voltage was 3.7 kV, the capillary temperature was 350 °C, and the sheath and auxiliary gas flow rates were 25 and 8 units respectively, with MS data acquired at 2–20 min. Chromatograms were obtained in data-independent acquisition (DIA) mode (full-scan: scan range *m/z* 500–1400, resolution 60,000, automatic gain control (AGC) target 1×10^6, maximum injection time (maxIT) 100 ms; DIA: resolution 15,000, AGC target 2×10^5, maxIT auto, and stepped collision energy (CE) of 30, 60 and 80 eV at *m/z* 530, 590, 650, 710, 770, 830, 890, 950, 1010, 1070, 1130, 1190, 1250, 1310, and 1370 with isolation window 62 and default charge state 1) to obtain full-scan and DIA fragmentation spectra. Mass spectral data were also collected using a combined full scan (FS) and top-10 data-DDA method. Data was acquired as for DIA but with an exclusion list generated from a blank injection and an inclusion list from a publicly available database of MC *m/z* values (Miles and Stirling, 2018), except that maxIT was set to 100 ms and dynamic exclusion 5.0 s and "if idle pick others" were selected. The DIA and DDA chromatograms were extracted for product-ions at *m/z* 135.0804, 135.1168, 361.1758, 375.1914, and 393.2020 to identify candidate MCs. Targeted LC–MS/MS spectra were obtained with alternating full-scan (as described above) and parallel reaction monitoring modes at the desired value of *m/z*, typically with resolution 30,000, AGC target 5×10^5, max IT 400 ms, isolation window 0.7. Typical collision energies were: stepped CE at 30 and 35 eV for MCs with no Arg; stepped CE at 60, 65 and 70 eV for MCs with one Arg; and CE at 65 eV for $[M+H]^+$ and stepped CE at 20, 25 and 30 eV for $[M+2H]^{2+}$ of MCs with two Arg groups. The resolution, maxIT, AGC target and injection volume were sometimes adjusted for minor peaks or insufficiently resolved product-ions, and the CE was sometimes adjusted (as specified) to enhance the intensity of structurally diagnostic product ions.

In negative mode the MS was calibrated from *m/z* 74–1922 and the spray voltage was −3.7 kV, while the capillary temperature, sheath and auxiliary gas flow rates were the same as for positive mode. Chromatograms were obtained in negative DIA mode (full scan: scan range *m/z* 750–1400, resolution 60,000, AGC target 1×10^6, maxIT 100 ms; DIA: scan range *m/z* 93–1400, resolution 15,000, AGC target 2×10^5, maxIT auto, and stepped CE 65 and 100 eV at *m/z* 772, 815, 858, 902, 945, 988, 1032, 1075, 1118, 1162, 1205, 1248, 1294, 1335, and 1378 with isolation window 45 and default charge state 1) to obtain full-scan and DIA fragmentation spectra. Mass spectral data were also collected using a combined full scan (FS) and top-10-DDA method. DDA data were acquired as for DIA but with an exclusion list generated from a blank injection and an inclusion list from a publicly available list of MC *m/z* values (Miles and Stirling, 2018), except that maxIT was set to 100 ms and dynamic exclusion 5.0 s and "if idle pick others" were selected. The DIA and DDA chromatograms were extracted for the product-ion at *m/z* 128.0353 to identify candidate MCs.

Dedicated full-scan chromatograms were obtained as described above, but with alternating positive and negative ionization scans with

the resolution set to 120,000 and maxIT to 300 ms. The positive-ion chromatograms of crayfish extracts were extracted for the exact *m/z* values (±5 ppm) for $[M+2H]^{2+}$ (**1**–**5**, **7** and **36**) or $[M+H]^{+}$ (**6**, **8**–**35**, **37** and **38**) ions of the microcystins in Table 1. A mixed quantitative standard containing MC-RR (**5**), MC-LR (**12**), and [Leu^1]MC-YR (113, 1023, and 393 ng/mL, respectively) was prepared from the CRMs and used to produce linear calibration curves (all $R^2 > 0.997$) from five serial 3-fold dilutions in MeOH. Peak areas from microcystins in the samples were then quantitated against the calibration curve for the most appropriate of the three external microcystin standards. Doubly-charged variants **1**–**5**, **7** and **36** were quantitated against $[M+2H]^{2+}$ of MC-RR, singly charged mono-Arg-containing variants **6** and **8**–**12** were quantitated against $[M+H]^{+}$ of MC-LR, and singly charged non-Arg-containing variants **13**–**35** against $[M+H]^{+}$ of [Leu^1]MC-LY).

2.7. Derivatization reactions

Mercaptoethanol derivatization was performed by addition of $(NH_4)_2CO_3$ (0.1 M, 200 μL) to filtered extracts (200 μL) followed by 1 μL of a 1:1 mixture of mercaptoethanol and d_4-mercaptoethanol (Sigma–Aldrich, St. Louis, MO, USA) (Yilmaz et al., 2019). A control reaction was performed in parallel whereby 1 μL of water was added instead of the thiol. Derivatization with Cys was performed by addition of $NaHCO_3$ (10 mg/mL, 10 μL) to an aliquot of extract (20 μL), followed by addition of L-cysteine (10 mg/mL, 10 μL). Oxidation of sulfide-containing MC variants, performed by addition of DMSO (10 μL) to an aliquot of the extract (25 μL) followed by addition of Oxone (10 mg/mL, 20 μL), was based on Miles et al. (Miles, 2017; Miles et al., 2014). Acetylation was performed by evaporation of an aliquot of the crayfish extract (50 μL) under N_2, adding acetic anhydride (10 μL) and pyridine (10 μL) and allowing the reaction to stand for 30 min, after which the reaction mixture was evaporated under N_2 and reconstituted in MeOH–H_2O (1:1, 50 μL).

2.8. Isotopologue analyses

The five most intense peaks in the $[M-H]^{-}$ and either $[M+H]^{+}$ or $[M+2H]^{2+}$ isotopologue clusters from LC–HRMS of putative MCs were analysed with the NRC Molecular Formula Calculator (version Oct 2022; https://metrology.shinyapps.io/molecular-formula-calculator/).

Table 1
Microcystins detected by LC–HRMS in water or crayfish samples from Lake Steinsfjorden in 2015 and 2016 (see also Fig. 1).[a]

#	Microcystin variant	RT (min)	Thiol react.[b]	Neutral Formula	Positive (z = +1 or +2)			MC profile of water (%)		
					z	Measured *m/z*	Δ (ppm)	2015		2016
								Jun	Sep	Oct
1	[D-Asp^3,Mlan^7]MC-RR	3.65	No	$C_{51}H_{80}O_{14}N_{14}S$	2	573.2926	0.7	0	0	0
2	[D-Asp^3,Mlan^7]MC-RR	4.11	No	$C_{51}H_{80}O_{14}N_{14}S$	2	573.2919	−0.7	0	0	0
3	[D-Asp^3]MC-RR	4.63	Yes	$C_{48}H_{73}O_{12}N_{13}$	2	512.7816	−1.5	65	78	7
4	[D-Asp^3,Dhb^7]MC-RR	4.70	No	$C_{48}H_{73}O_{12}N_{13}$	2	512.7826	0.5	20	22	7
5	MC-RR	4.72	Yes	$C_{49}H_{75}O_{12}N_{13}$	2	519.7898	−0.7	0	0	2
6	[DMAdda^5]MC-LR	6.11	Yes	$C_{48}H_{72}O_{12}N_{10}$	1	981.5385	−2.0	0	0	0
7	[Mlan^7]MC-LR	6.44	No	$C_{52}H_{81}O_{14}N_{11}S$	2	558.7904	−2.1	0	0	0
8	[D-Asp^3,Dhb^7]MC-HtyR	7.15	No	$C_{52}H_{72}O_{13}N_{10}$	1	1045.5359	0.6	2	0	15
9	[D-Asp^3,Dhb^7]MC-LR	7.26	No	$C_{48}H_{72}O_{12}N_{10}$	1	981.5428	2.5	12	0	29
10	[D-Asp^3]MC-LR	7.19	Yes	$C_{48}H_{72}O_{12}N_{10}$	1	981.5409	0.5	2	0	23
11	[Dha^7]MC-LR	7.43	Yes	$C_{48}H_{72}O_{12}N_{10}$	1	981.5375	−3.0	0	0	7
12	MC-LR	7.40	Yes	$C_{49}H_{74}O_{12}N_{10}$	1	995.5549	−1.1	0	0	2
13	[Mlan^7]MC-LHnv[c]	9.85	No	$C_{51}H_{78}O_{15}N_8S$	1	1075.5383	0.3	0	0	0
14	[Mlan^7]MC-LHnv[c]	10.15	No	$C_{51}H_{78}O_{15}N_8S$	1	1075.5387	0.7	0	0	0
15	[DMAdda^5]MC-LHnv	10.97	Yes	$C_{47}H_{69}O_{13}N_7$	1	940.5034	0.8	0	0	0
16	MC-LCit	12.22	Yes	$C_{49}H_{72}O_{13}N_9$	1	996.5377	−2.4	0	0	0
17	[D-Asp^3]MC-LHnv	12.28	Yes	$C_{47}H_{69}O_{13}N_7$	1	940.5001	−2.7	0	0	0
18	[Mser^7]MC-LHnv	12.48	No	$C_{48}H_{73}O_{14}N_7$	1	972.5290	0.2	0	0	0
19	dmMC-LHnv	12.60	Yes	$C_{47}H_{69}O_{13}N_7$	1	940.5022	−0.4	0	0	0
20	MC-LM(O)	12.70	Yes	$C_{48}H_{71}O_{13}N_7S$	1	986.4895	−0.8	0	0	0
21	[Dha^7]MC-LHnv	12.85	Yes	$C_{47}H_{69}O_{13}N_7$	1	940.5015	−1.2	0	0	0
22	MC-LNao	13.00	Yes	$C_{50}H_{74}O_{13}N_8$	1	995.5428	−2.0	0	0	0
23	[Glu(OMe)^6]MC-LHnv	13.08	Yes	$C_{49}H_{73}O_{13}N_7$	1	968.5339	0.0	0	0	0
24	dmMC-LHnv	13.30	Yes	$C_{47}H_{69}O_{13}N_7$	1	940.5013	−1.4	0	0	0
25	MC-LHnv	13.34	Yes	$C_{48}H_{71}O_{13}N_7$	1	954.5172	−1.2	0	0	0
26	MC-HilHnv	13.76	Yes	$C_{49}H_{73}O_{13}N_7$	1	968.5352	−1.0	0	0	0
27	MC-LA	14.80	Yes	$C_{46}H_{67}O_{12}N_7$	1	910.4916	−0.5	0	0	0
28	MC-LY	15.12	Yes	$C_{52}H_{71}O_{13}N_7$	1	1002.5175	−0.7	0	0	0
29	MC-LAbu	16.00	Yes	$C_{47}H_{69}O_{12}N_7$	1	924.5065	−1.3	0	0	0
30	MC-LM	16.60	Yes	$C_{48}H_{71}O_{12}N_7S$	1	970.4943	−1.2	0	0	0
31	MC-LW	16.97	Yes	$C_{54}H_{72}O_{12}N_8$	1	1025.5326	−1.6	0	0	0
32	MC-LV	16.97	Yes	$C_{48}H_{71}O_{12}N_7$	1	938.5214	−2.1	0	0	0
33	MC-LF	17.54	Yes	$C_{52}H_{71}O_{12}N_7$	1	986.5221	−1.3	0	0	0
34	MC-LL	17.83	Yes	$C_{49}H_{73}O_{12}N_7$	1	952.5376	−1.5	0	0	0
35	MC-LL isomer	17.96	Yes	$C_{49}H_{73}O_{12}N_7$	1	952.5379	−1.2	0	0	0
36	[Dha^7]MC-RR[d]	–	Yes	$C_{48}H_{73}O_{12}N_{13}$	2	–	–	0	0	3
37	[D-Asp^3]MC-HtyR[d]	–	Yes	$C_{52}H_{72}O_{13}N_{10}$	1	–	–	0	0	5
38	[Dha^7]MC-HtyR[d]	–	Yes	$C_{52}H_{72}O_{13}N_{10}$	1	–	–	0	0	1

[a] A fuller version of Table 1 is presented in Table S1, including negative ionization mode results. Retention times and mass errors are from representative LC–HRMS analyses. Variants **13**–**26** and **35** do not appear to have been reported previously. Variants **1**, **2**, **7**, **13**, **14**, and **30** reacted with mild oxidants (**30** reacted to give **20**) to give the corresponding sulfoxides while the remaining variants were unreactive. An additional partially characterized variant with *m/z* 972.5288 (**25** + H_2O) was also detected at 10.92 min (Table S3). "MC profile of water (%)" is the percentage of the total MCs detected in that month's sample.

[b] Thiol. react. = reacted rapidly with mercaptoethanol under weakly basic conditions.

[c] **13** is the minor isomer, **14** is the major one.

[d] Only detected indirectly by mercaptoethanol derivatization, due to chromatographic overlap of the underivatized compound with major isomer(s).

Elemental constraints used were: C, 40–60; H, 50–100; N, 7–14; O, 12–18, and S, 0–1 (based on Miles and Stirling (2019)), usually with the "Use Senior Rules" setting with the mass tolerance set to 5 ppm and resolution set to 0.001 *m/z*. With these settings, generally only one viable elemental formula was obtained with a realistic number of rings plus double-bond equivalents (RDBE) (16–30) from examining both the positive and negative mode spectra. An illustrative example of this approach is shown for the putative novel MC metabolite MC-LHnv (**25**) (Figs. S1 and S2), for which the only neutral formula satisfying the abovementioned constraints was $C_{48}H_{71}O_{13}N_7$.

3. Results and discussion

In this study we demonstrate that the high levels of MCs in crayfish in Lake Steinsfjorden during the autumn, when the levels of MCs in the water were low, not only remained high, but that the toxin profile changed dramatically to a suite of variants that were at no stage present in the water column. Below, we present these results and discuss their implications.

3.1. Strategy for identification of candidate MCs by LC–HRMS/MS

A strategy designed to detect the widest possible array of MCs by LC–HRMS was applied to the extracts, including analysis in full-scan mode with alternating positive and negative ion scans, in conjunction with mercaptoethanol derivatization to identify thiol-reactive potential Mdha^7-and Dha^7-containing MC variants. In addition to this, LC–HRMS/MS was performed using DIA and DDA in both positive and negative ionization modes. The negative mode DIA and DDA chromatograms were extracted for the product-ion D-Glu^6 moiety (Fig. 1) present in all toxic MCs, and the positive mode DIA and DDA chromatograms were extracted for a range of characteristic product ions arising from the Adda^5-moiety and from the Adda^5–D-Glu^6–Dha^7/Mdha^7/Mser^7 moieties (Fig. 1). This strategy was, therefore, expected to detect any MC variants containing the amino acids previously detected at positions-5 and -6, and most of the known variants at position-7, and thus to have the potential to detect essentially any toxic MC regardless of its amino acid composition at the more variable positions 1–4 (Fig. 1).

Previous studies have shown the MC profile in Lake Steinsfjorden to be dominated by toxins from *Planktothrix* spp. The MCs from Lake Steinsfjorden, or from *Planktothrix* cultures isolated from it, produce either Dhb^7-or Mdha^7-containing D-Asp^3-variants of MCs (Mallia et al., 2019; Miles et al., 2013a). The lakewater typically contains a mixture of isomeric pairs of Dhb^7-and Mdha^7-variants of [D-Asp^3]MCs, produced by cohabiting strains of *Planktothrix* (Miles et al., 2013a). As these isomeric MCs have nearly identical retention times and fragmentation patterns in most LC–MS methods, the most practical way to differentiate between them with certainty by LC–MS is via their substantially different reactivity with thiols (Miles et al., 2013a). We applied this approach by derivatizing samples with a 1:1 mixture of mercaptoethanol and d_4-mercaptoethanol, which reacts rapidly with Dha^7- and Mdha^7--containing MCs, but hundreds of times more slowly with the more sterically hindered olefin in Dhb^7-containing MCs. Not only is this change readily detected by LC–MS, but the derivatization products are also easily identified from their characteristic isotopologue profiles (peaks separated by m/z 4.0251 or 2.0126 for $z = \pm1$ or $z = \pm2$, respectively; e.g. see Fig. S3) by LC–HRMS (Mallia et al., 2019), and have similar LC–MS responses to their underivatized precursors (Miles et al., 2013a). This approach was applied to analyse both the water samples from Lake Steinsfjorden and selected crayfish extracts, and its application is exemplified by the analysis of the MCs in the water in June 2015 (Fig. 3). Fig. 3F shows the underivatized MC profile, including unresolved peaks for the isomeric pairs **3** and **4**, and **9** and **10**. However, after derivatization, the underivatized Dhb^7-MCs **4**, **8** and **9** remained (Fig. 3A, C, and E), whereas Mdha^7-MCs **3** and **10** disappeared and were replaced by their corresponding thiol derivatives (**3*** and **10***, respectively, in

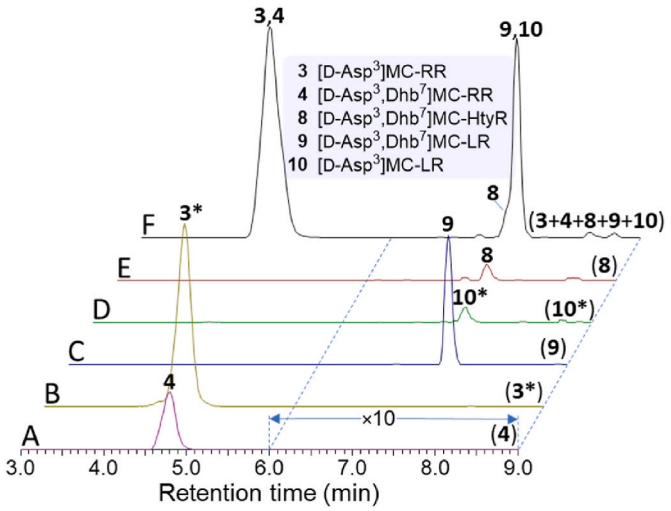

Fig. 3. Thiol derivatization of the extract from filters collected from water at 0–22 m in June 2015. LC–HRMS full-scan extracted-ion chromatograms (positive mode, ±5 ppm) A–E are from the sample after derivatization with 1:1 mercaptoethanol and d_4-mercaptoethanol (i.e. Mdha^7-MCs are derivatized, but Dhb^7-MCs are not), extracted at: A, m/z 512.7824 (**4**); B, m/z 551.7893 and 553.8019 (**3** derivatized with mercaptoethanol, i.e. **3***); C, m/z 981.5404 (**9**); D, m/z 1059.5543 and 1063.5794 (**10** derivatized with mercaptoethanol, i.e. **10***), and; E, m/z 1045.5353 (**8**). Chromatogram F is from the same sample without thiol derivatization, and is the sum of extracted ions at m/z 512.7824 (**3** and **4**), 981.5404 (**9** and **10**), and 1045.5353 (**8**). No other MCs were detected in this sample, apart from trace levels of the two isomeric cysteine conjugates of **3** (**1** and **2**). The derivatization chromatograms (A–E) are scaled to intensity of the peak for **3** + **4** in chromatogram F (the underivatized control sample), and the intensities from 6 to 9 min are expanded 10-fold to help visualize the minor MCs in the sample. MCs variants detected as mercaptoethanol derivatives (i.e. containing Dha^7 or Mdha^7) are marked with asterisks.

Fig. 3B and D). Thiol derivatization was also helpful for identifying Mser^7/Ser^7-containing MCs, and MCs conjugated to Cys (or GSH), because these variants do not contain a thiol-reactive conjugated olefin at position-7 (Fig. 1).

The identities of putative Cys conjugates of MCs (i.e. Mlan^7-variants) were verified by semisynthesis via reaction of selected extracts with Cys under weakly basic conditions (Kondo et al., 1992), followed by LC–HRMS comparison with extracts containing the putative Cys conjugates. As with the mercaptoethanol derivatization, this reaction with Cys was rapid for Mdha^7-and Dha^7-containing MCs (Fig. S4), whereas the corresponding Dhb^7-variants reacted only very slowly. The presence of MCs containing sulfide linkages (i.e. Cys conjugates of MCs, and MC-LM (**30**)) in extracts was confirmed by mild oxidation with DMSO/Oxone (Miles, 2017), which oxidizes sulfides to sulfoxides. This reaction results in a characteristic increase in mass for the sulfoxide product of 15.9949 Da, and a shortening of the retention time, relative to the sulfide-containing precursor, when compared to the underivatized sample by LC–HRMS (Fig. S4).

3.2. Identification of individual MC variants

Many of the MCs were identified by comparison of their retention times, product-ion spectra and chemical reactivities with those of MC standards (**3**, **4**, **10**–**12**, **27**, **28**, **31**, and **33**) or with culture- or field-samples in which these compounds had been reported (**1**, **2**, **6**–**9**, **29**, **32**, and **34**). All the MCs reported in Table 1 reacted rapidly with mercaptoethanol, except for those containing Dhb^7 (**4**, **9**), Mser^7 (**18**), or those that were found to be Cys conjugates (**1**, **2**, **7**, **13**, and **14**) of Mdha^7-containing MCs, which were all unreactive toward mercaptoethanol. MCs that contained sulfide moieties (**1**, **2**, **7**, **13**, **14**, and **30**) were oxidised to their sulfoxides by Oxone/DMSO, while the remaining

MCs, including sulfoxide-**20**, were not affected. The identities of the minor Cys conjugates MCs (**1**, **2**, **7**, **13**, and **14**) were further confirmed by reaction of the sample with Cys under basic conditions, to convert the more abundant unconjugated MCs (**3**, **12**, **25**) to their semisynthetic Cys-conjugates.

Crayfish samples from later in the summer of 2015 contained many MCs that were not detected in the corresponding water samples. These included MC-LR (**12**), but in some cases there were much larger peaks of later-eluting MCs, some of which appeared to be metabolites. A thiol-reactive peak eluting at 12.22 min had accurate masses and thiol reactivity consistent with MC-LCit (**16**). Low levels of [D-Asp^3]MC-RCit were recently reported in a culture of *Planktothrix prolifica*, and were suspected to have been produced from the much more abundant [D-Asp^3]MC-RR (**3**) that was present (Mallia et al., 2019). Confirmation of the identity of **16** was obtained by comparison of its LC–HRMS/MS spectrum with that of MC-LA (**27**) (Figs. S5–11, Table S2). This showed that the difference in mass between MC-LA and **16** was located solely on the side-chain of the amino acid at position-4. Furthermore, the LC–HRMS/MS spectrum of $[M+H]^+$ of **16** showed a neutral loss of HNCO (43.0058 Da) from the terminal ureido moiety, characteristic of Cit-containing peptides (Hao et al., 2009).

A prominent thiol-reactive peak (**25**) eluting at 13.61 min in extracts from crayfish in late summer had accurate masses and an isotope profile consistent with $C_{48}H_{71}N_7O_{13}$. Comparison of its product-ion spectrum with that of MC-LA (**27**) (Figs. S12–S16, Table S2) revealed that the mass difference was located entirely in the amino acid at position-4, and this amino acid therefore had the neutral elemental composition $C_5H_{11}NO_3$, containing 1 RDBE. Given that only L-amino acids have ever been identified at position-4 in MCs, it seemed likely that this was a hydroxylated L-amino acid not previously reported in MCs. Consistent with this, several of the expected product-ions containing amino acid-4 were dehydrated (loss of 18.0106 Da) relative to the expected *m/z* value. Hydroxylation was confirmed by derivatization of an extract with acetic anhydride to give the monoacetate derivative. Analysis of the resulting acetate's product-ion spectrum confirmed the acetate to also be located at position-4 (Table S2). These results are consistent with the presence of the uncommon L-amino acid 5-hydroxynorvaline (Hnv), which has been reported in both plants and bacteria (Hill et al., 1993; Yan et al., 2014), although hydroxylation at other locations on the amino acid side-chain cannot be excluded from the mass spectral data. However, the co-occurrence of **25** in crayfish with MC-LR (**12**) and MC-LCit (**16**) suggests that **25** may be produced by hydrolytic or other metabolic processes in the crayfish (Fig. 4) from one of these, and is therefore tentatively identified as MC-LHnv (**25**). The diastereomeric pair of Cys adducts of MC-LHnv (**13** and **14**) were also present in the crayfish extracts in late summer. Their identities were confirmed by their accurate masses, isotope profiles, LC–HRMS/MS spectra, their ready oxidation to their sulfoxides, and semisynthesis (Figs. S4 and S17). A number of minor derivatives of MC-LHnv (**25**) were detected by LC–HRMS/MS in the crayfish, including the Mser^7-derivative (**18**), five demethylated congeners (**15**, **17**, **19**, **21**, and **24**), and a methylated variant (**26**). The demethylated variants were not identified with certainty due to limited signal-to-noise in their product-ion spectra (Fig. S18), but appear to include the DMAdda^5-, D-Asp^3-, and Dha^7-congeners of MC-LHnv (**15**, **17**, and **21**, respectively) based on relative retention times and product-ion spectra (Fig. S18). Similarly, the [Mser^7]MC-LHnv (**18**) showed relatively low signal-to-noise (Fig. S19, Table S2), but included a prominent product ion at *m/z* 393.2014 consistent with the presence of *N*-methylserine at position-7. A second, broader and earlier-eluting isomer of **18** was detected at 10.92 min, displaying a product-ion at *m/z* 135.0804, but the signal-to-noise ratio in the spectrum was insufficient for further identification. A slightly later-eluting methylated variant (**26**) of **25** was also detected, and detailed examination of its LC–MS/MS spectrum (Figs. S20–23, Table S2) showed that it contained an extra CH_2 group in the amino acid at position-2, relative to MC-LHnv. This methylated variant was, therefore, tentatively identified as MC-HilHnv (**26**).

A later-eluting, thiol-reactive, minor MC (**22**) in the crayfish extracts from late summer had *m/z* 995.5, but its accurate mass and isotopologue profile showed its formula to be $C_{50}H_{74}N_8O_{13}$. Consistent with this, the retention time, adduct-ion profile, and product-ion spectrum were indicative of an MC that did not contain Arg. Comparison of the product-ion spectrum of **22** with that of MC-LA (**27**) obtained under the same conditions (Figs. S24–27, Table S2) showed that the entire mass difference between the two MCs was located on the amino acid at position-4. This amino acid, therefore, has the elemental composition $C_7H_{14}N_2O_3$, containing 2 RDBE, and did not contain a hydroxy or amino group (as **22** did not undergo acetylation when the extract was treated with acetic anhydride as described above). The amino acid at position-4 is, therefore, probably N^5-acetylornithine (Fig. 4), given that this amino acid has been reported as a plant and animal metabolite (Armstrong, 1979), and that apparent metabolites of MC-LR (**12**) appeared to be abundant in the crayfish at this time.

MC-LM (**30**) and a trace of MC-LM(O) (**20**) were detected in crayfish with the appropriate accurate masses (Table 1). As no standard of **30** was available, and **20** has not been reported before, their identities were confirmed by chemical reactions and comparison of their LC–HRMS/MS spectra with those of MC-LA (**27**) (Figs. S28–32, Table S2). Both compounds reacted rapidly with mercaptoethanol, indicating the presence of Mdha^7 or Dha^7. Mild oxidation with Oxone/DMSO completely converted sulfide **30** into its sulfoxide derivative, **20**. Examination of the LC–HRMS/MS spectra confirmed the sequence of the seven amino acids in both compounds, and revealed that **20** showed a neutral loss of CH_3SOH that is characteristic of peptides containing a terminal methyl sulfoxide (Jiang et al., 1996; Miles et al., 2014), thus confirming the identities of both **20** and **30**.

3.3. Microcystin profiles in Lake Steinsfjorden

Five significant MCs (**3**, **4**, and **8**–**10**), together with trace levels of

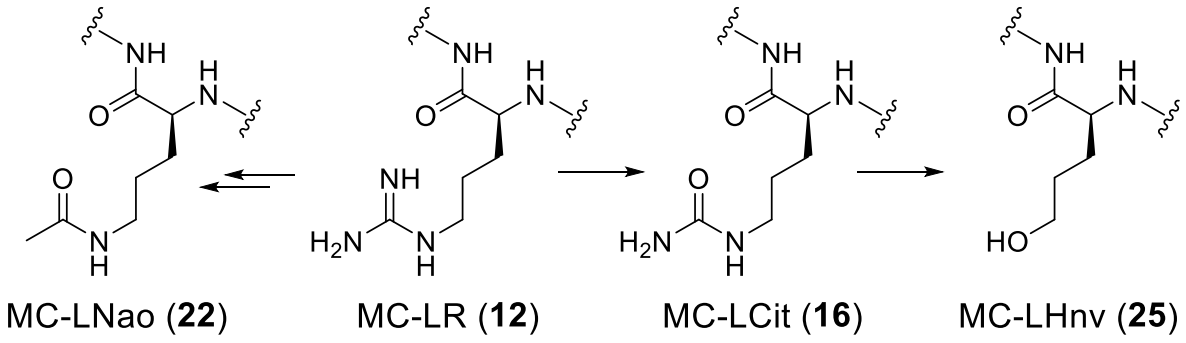

Fig. 4. Structures, and possible routes for formation, of MC-LCit (**16**), MC-LNao (**22**), and MC-LHnv (**25**) from MC-LR (**12**). Enzymatic citrullination of Arg-containing peptides and proteins is well known (Flores et al., 2019; Mondal and Thompson, 2019).

two isomeric Cys conjugates, were detected in extracts of filters taken monthly (0–20 m) from Lake Steinsfjorden during spring and early summer 2015, during the *Planktothrix* bloom. Both [D-Asp^3]MC-RR (**3**) and its isomeric variant [D-Asp^3,Dhb^7]MC-RR (**4**) were present, in a ratio of about 3:1 throughout the study period in 2015, as revealed by derivatization with mercaptoethanol (Fig. 3, Table 1). Much lower levels of [D-Asp^3,Dhb^7]MC-LR (**9**) and its isomer [D-Asp^3]MC-LR (**10**) (about 5:1) were also present in May–July, along with trace amounts of [D-Asp^3, Dhb^7]MC-HtyR (**8**) (Fig. 3, Table 1). Although the LC–HRMS analysis was only semiquantitative, the intensities of peaks for MCs identified by LC–HRMS (Fig. 5) paralleled the quantitation obtained by ELISA from integrated water samples (Fig. 2), with the total content of MCs reaching its lowest levels in August (Figs. 2 and 5, and Fig. S33). No other MCs were detectable in the filter extracts despite the use of untargetted LC–HRMS and thiol derivatization methods. Previous studies of cultures have shown that *Planktothrix* strains produce either Mdha^7-or Dha^7-MCs (Kurmayer et al., 2005; Miles et al., 2013a). Therefore, these results suggest the presence of at least two strains of different chemotypes during the study period in 2015: a dominant chemotype producing the Mdha^7-variant [D-Asp^3]MC-RR (**3**) and a trace of [D-Asp^3]MC-LR (**10**), and a second chemotype producing Dhb^7-variants **4**, **8**, and **9**. Interestingly, a sample taken in September 2016 contained the D-Asp^3, Dhb^7-variants **4**, **8**, and **9**, and D-Asp^3,Mdha^7-variants **3**, **11**, and **37**, presumably from two *Planktothrix* chemotypes, and low levels of the Mdha^7-variants **5** and **12** (Fig. 3, Fig. S34, Table 1), possibly from *Microcystis viridis*, another potentially MC-producing cyanobacterium that was present in low levels in the September water sample (3.6 mg/m^3). This indicates that the dominant chemotype of *Planktothrix* in Lake Steinsfjorden varies with time but is not purely seasonal, and that other genera appear to occasionally contribute to the MC profile in the lake.

3.4. Microcystin profiles in the crayfish

MCs were detected in all 110 individuals of noble crayfish collected from Lake Steinsfjorden in 2015 and 2016 with the multihapten MC-ELISA (Samdal et al., 2020). MC-profiles by LC–HRMS were obtained from the tail muscles, hepatopancreata, intestines and stomachs of the five most heavily contaminated crayfish, as judged by the multihapten-ELISA, collected each month. Individual crayfish from any given harvesting time-point varied in the concentrations of MCs present, but had similar MC-profiles in their tissues. Therefore the profiles will be described in general for June and September 2015, and illustrated with results from the two most heavily contaminated individual animals for those time-points. The stomachs generally contained the highest concentrations of MCs (Samdal et al., 2020), so MC profiles obtained from the stomachs were used for comparisons between individual animals and sampling times.

The crayfish from June contained three main MCs, two MC-RR-variants (**3** and **4**) and one MC-LR-variant (**9**). The MC profiles were similar in all tissues (tail muscle, stomach, intestine and hepatopacreas) from the same crayfish (Fig. 6), and generally corresponded well with the observed MCs in the filters from the water (Figs. 5–7) although some MC-LR (**12**) and low levels of later eluting MCs were detected in some individuals (Fig. 7). The correspondence between MCs in the crayfish and in the filters from the water indicated that the MCs in the crayfish in May and June originated primarily from the water, and most likely from the observed *Planktothrix* bloom. The crayfish from July (Fig. S35) contained the same three main MCs as the crayfish in June and as found in the water. However, in addition, five other significant MCs were also detected in some individuals, among them MC-LR (**12**), three putative MC-LR metabolites (**14**, **16** and **25**) and MC-LA (**27**).

The MC profiles of crayfish from August (Fig. S36), September (Figs. 6 and 7) and October (Fig. S37) of 2015 were dominated by MCs that were not detected in the water column, although low levels of [D-Asp^3]MC-RR-variants **3** and **4** were present in two individuals in October. The same MC-profile was observed in all tissues from the same individual crayfish in September (Fig. 6), so the profile from the stomach content is representative and could be compared to the MC profile of the water. LC–HRMS-chromatograms revealed that MC variants **3** and **4**, present in the water at low levels (Fig. 5E), were present only at trace levels in the crayfish stomachs in September 2015 (Fig. 7, Table S3). In contrast, neither MC-LR and its putative metabolites (**12**–**14**, **16**, **22** and **25**), nor the known later-eluting cyanobacterial MC variants (**27**–**35**), were detected in any of the water samples in 2015, despite these and related variants being the dominant MCs in the stomach contents in September. These results indicate that almost none (less than 1%, according to Table S3) of the MCs in the crayfish in late summer and autumn of 2015 originated from the *Planktothrix* present in Lake Steinsfjorden at that time.

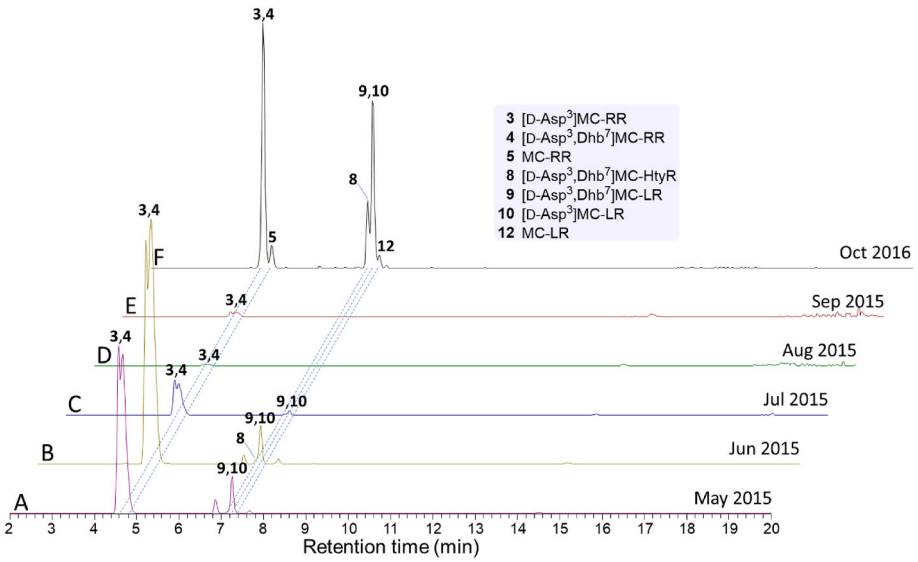

Fig. 5. Microcystins extracted from filters from water collected from 0 to 22 m in Lake Steinsfjorden. The water samples are from May to September 2015 and October 2016 and shown as LC–HRMS chromatograms (positive mode, sum of extracted ions for **3**, **4**, **5**, **8**, **9**, **10** and **12** at *m/z* from Table 1). Peak-label numbers refer to microcystin variants in Fig. 1 and Table 1. The intensities of the five chromatograms from 2015 are scaled relative to the sample collected in June. Blue dashed lines show retention times of MCs present at significant levels primarily in the water.

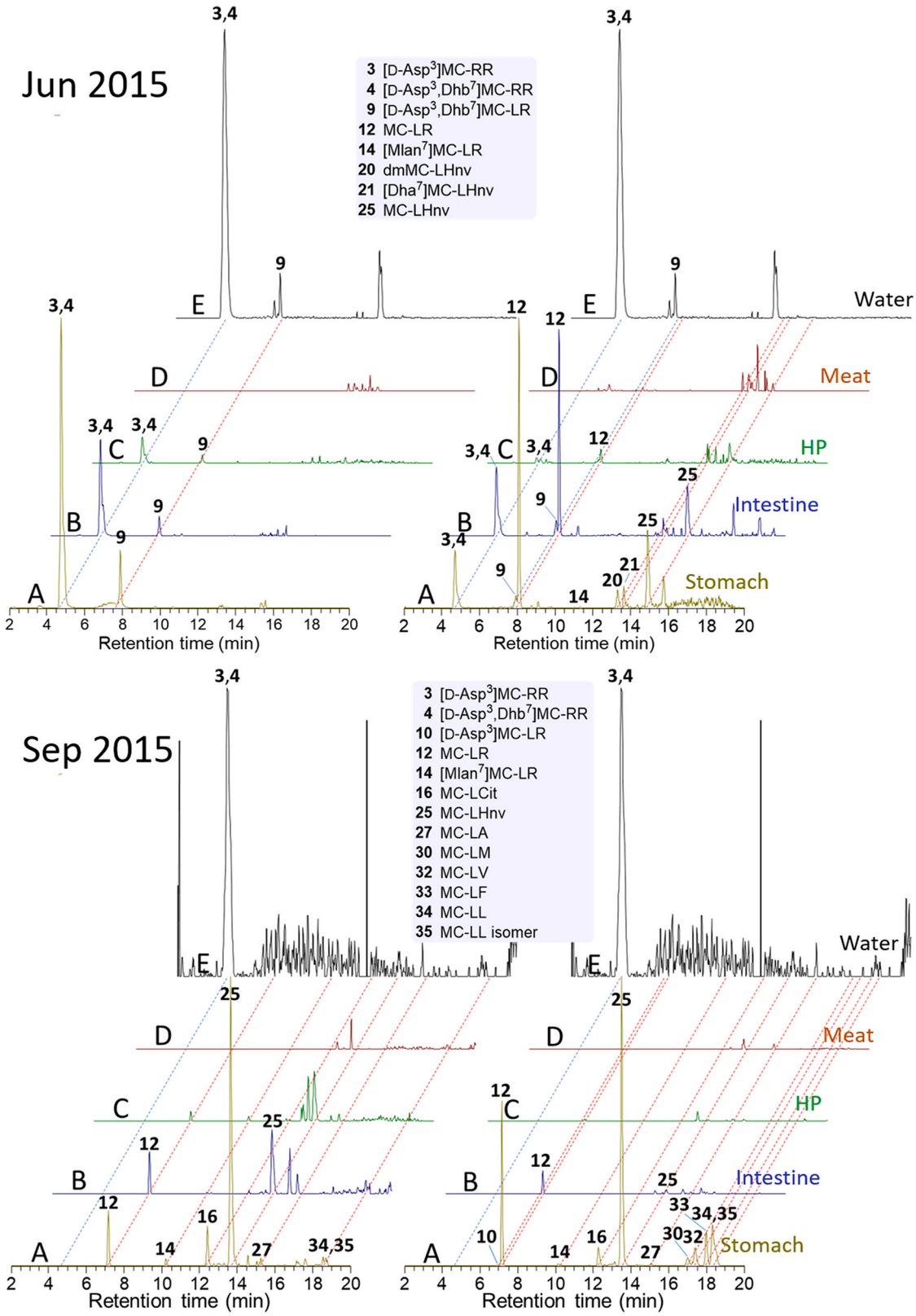

Fig. 6. LC–HRMS extracted ion chromatograms (positive mode, summed for all MC ions in Table 1) of four tissue samples from each of the two crayfish with the highest concentrations of MCs by multihapten-ELISA harvested in: top, June 2015, and; bottom, September 2015. Chromatograms for each animal are for: A, stomach contents; B, Intestine; C, hepatopancreas, and; D, tail meat without intestine. Chromatogram E shows MCs detected on filters in the water at harvest time. The major MCs are indicated with compound-numbers (Table 1 and Fig. 1). Chromatograms of extracts of crayfish tissues (A–D) are normalised to the maximum intensity in the extract from the stomach contents for each animal, and so are indicative of the relative concentrations MCs in the tissues of each individual. Blue and red dashed lines show retention times of MCs present at significant levels primarily in the water, or in the crayfish, respectively.

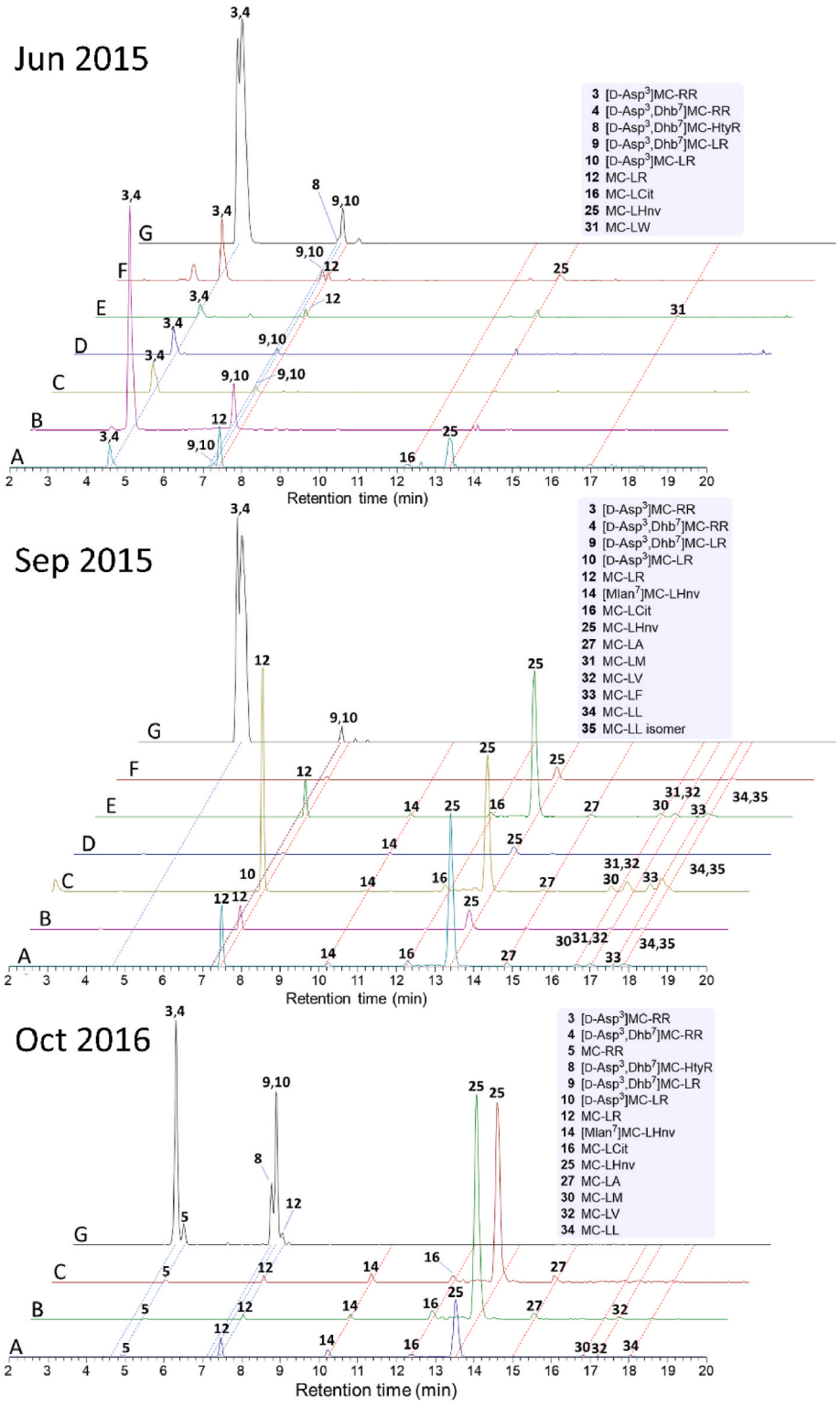

Fig. 7. Microcystin stomach contents from the three to six individual crayfish with the highest concentrations of MCs by multihapten ELISA, harvested: top, in June 2015 (A–F); middle September 2015 (A–F), and; bottom; October 2016 (A–C), compared with MCs detected in the water (chromatogram G for each month) at the time of harvest, shown as LC–HRMS extracted ion chromatograms (positive mode, summed for all MC ions in Table 1). Major MCs are indicated with compound-numbers from Table 1 and Fig. 1. Chromatograms of extracts of crayfish stomach contents are normalised to the individual with the maximum intensity in each month, and so are indicative of the relative concentrations of MCs in each of the three to six individuals. Blue and red dashed lines show retention times of MCs present at significant levels primarily in the water, or in the crayfish, respectively.

Interestingly, MC-LR (**12**) and MC-RR (**5**) were detected by LC–HRMS at low levels in a water sample taken from Lake Steinsfjorden the following year, in October 2016, although the toxin profile was dominated by [D-Asp^3,Dhb^7]-variants **4**, **8** and **9**, with the corresponding [D-Asp^3,Mdha^7]-variants (**3**, **10** and **37**) also present (Fig. 5 and Fig. S34, Table 1 and Table S1). This is the first report of MC-RR and MC-LR in water from Lake Steinsfjorden, and may reflect a low-density bloom of *Microcystis* or some other non-*Planktothrix* spp., although the overall concentrations of cyanobacterial cells in the water column were low at the time in question (Fig. 2 and Fig. S33). Stomachs from crayfish harvested in October 2016 contained elevated levels of MCs (Table 1 of Samdal et al. (2020)) according to the multihapten MC-ELISA, despite the relatively low levels of MCs in the water. LC–HRMS analysis of stomachs from the three crayfish with the highest levels of MCs by ELISA from October 2016 (Fig. 7) showed only trace levels of most of the MCs that were present in the water column, closely paralleling the finding from 2015. However, the toxin profiles in these crayfish samples were dominated by the putative MC-LR-metabolite MC-LHnv (**25**), its Cys-conjugates (**13** and **14**), and MC-LCit (**16**) together with low levels of MC-LR (**12**) and a range of other known non-Arg-containing MCs such as MC-LA (**27**), MC-LM (**30**) and MC-LL (**34**). These results suggest that different strains of *Planktothrix*, ones that predominantly produced variants **8**–**10** (rather than variants **3** and **4** as in 2015), may have become dominant in the water column in late summer 2016. Nevertheless, the pattern of MCs in the crayfish in October 2016 (Fig. 7) was similar to that in September 2015 (Fig. 7), with MCs not detected in the water—including presumed metabolites of MC-LR—being by far the most abundant, once again indicative of an alternative, non-planktonic source of MCs in the crayfish diet in the late summer in Lake Steinsfjorden.

MC production by two benthic cyanobacteria (*Nostoc linckia* and *Limnothrix mirabilis*) has been described in an Australian reservoir by Gaget et al. (2017), and Cantoral Uriza et al. (2017) have described MC production in Spanish benthic cyanobacterial strains from different habitats. Therefore, the possible presence of benthic cyanobacteria in Lake Steinsfjorden is worth investigating as a possible source of non-planktonic MCs. Without knowing the origin of the non-planktonic MCs found in the crayfish, measurements of the cyanobacterial biomass or MC content in the water column cannot reliably be used to make predictions about the presence of MCs in crayfish in Lake Steinsfjorden. The results indicate that such measurements on their own are therefore of limited value for food safety assessment for noble crayfish in this lake. Whether this also applies to other aquatic wildlife, or to other water bodies, remains to be determined.

An array of known (**1**–**12**, **27**–**35**) and novel (**13**–**26** and MC-LHnv + H_2O) MCs was identified in the crayfish by LC–HRMS (Fig. 1, Table 1 and Tables S1, S3). To verify that the majority of the MCs in the animals had been detected with the LC–HRMS method, the total concentrations of MCs in the stomachs of the 15 most heavily contaminated crayfish were estimated by LC–HRMS (Table S3), and compared to the concentrations measured with the multihapten MC-ELISA. Because quantitative standards were not available for most of the 39 MCs detected in the samples, concentrations were estimated against a CRM of the MC that each variant was considered to most closely resemble in terms of charge state and ionizability (**1**–**5**, **7**, and **36** against **5**; **6**, **8**–**14**, **37**, and **38** against **12**, and; **15**–**35** and MC-LHnv + H_2O against [D-Leu^1]MC-LY), and potential matrix effects were not corrected for. The crayfish with the highest levels of MCs by ELISA (454 μg/g in the stomach) as reported by Samdal et al. (2020) was measured at a much lower level of total MCs by LC–HRMS (25.9 μg/g (2589 ng/mL in the extract), Table S3), and was therefore excluded from this analysis as an outlier. The reason for this discrepancy is under investigation. Nevertheless, the results of this analysis (Fig. 8) showed an excellent correlation between the two methods, with the LC–HRMS results being about 75% of the ELISA results over the course of 5 months, during which time the toxin profiles in the crayfish changed markedly. The difference in the results from the two types of analysis may be due to variations in ELISA cross-reactivities and LC–HRMS response factors across the 39 MCs detected, matrix effects in the LC–HRMS that could not easily be corrected for, or to small amounts of multiple MC analogues detected collectively in the ELISA but individually below the detection limit in the LC–HRMS method. There could also be a contribution from MCs with characteristics that make them non-detectable with the current LC–HRMS method, such as protein- or other conjugates, very polar or non-polar variants, or variants with unusual charge states or *m/z* values, such that they are outside the retention time or *m/z* ranges used in the analysis. Nevertheless, if this is the case, then these undetected variants probably do not amount to more than about 25% of the total MCs detected by ELISA in the crayfish.

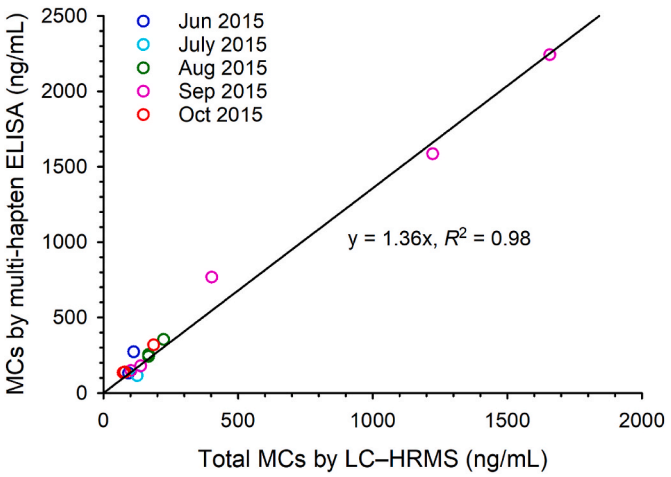

Fig. 8. Total MC concentrations in extracts of crayfish stomachs for 14 of the 15 crayfish, from Lake Steinsfjorden in Jun–Oct 2015, with the highest concentrations by the multihapten-ELISA. ELISA data are from Samdal et al. (2020), and LC–HRMS data are sums of the concentrations of all MCs detected in this study (i.e. **1**–**38** and "**25** + H_2O"; see Table 1, Tables S1, S3, and Fig. 1) as measured in positive ionization mode. The sample with the very highest level (S9–K07S–S9, Table S3) was excluded as an outlier. See Fig. S38 for additional analysis.

Furthermore, because the quantitative analysis of the stomach contents by ELISA correlated well with the LC–MS analysis when both the known and novel MCs were included, it seems likely that the food safety evaluation conducted by Samdal et al. (2020) based on the ELISA data for the edible parts (tail muscle and intestine) was appropriate.

The results of this study also illustrate the potential for obtaining misleading results when samples that may be rich in unexpected MC variants are analysed with highly targeted LC–MS methods. Although the untargeted LC–HRMS/MS and ELISA methods used in this study gave similar results (Fig. 8, Table S3), this would not have been the case if targeted LC–MS/MS methods had been used without prior knowledge of the microcystin profiles in the crayfish. For example, the "common" MCs (MC-RR (**5**), MC-LR (**12**), MC-YR, and MC-LA (**27**), or their isomeric Dhb^7-variants) that are most often reported and analysed for, constituted only between 11% (Oct 2015) and 40% (Aug 2015) of the MCs detected in crayfish stomachs in 2015 (Table S3). Even targeted LC–MS/MS analysis for every previously reported MC variant (Bouaïcha et al., 2019; Jones et al., 2021), which in these experiments would have detected **1**–**12** and **27**–**38**, would have resulted in total measured MC concentrations of between 13% (Oct 2015) and 87% (Jun 2015) of those detected by the untargeted LC–HRMS method used here. Such targeted LC–MS/MS analyses would have resulted in a substantial underestimation of the MC content in the crayfish, and in an apparently poor correlation between the ELISA and LC–MS results (Fig. S38).

4. Conclusions

A previous study of Lake Steinsfjorden in 2015 and 2016 showed no significant correlation between concentrations of MCs in crayfish and the water, despite there being a strong correlation between the concentrations of MCs (by ELISA) and *Planktothrix* cells in the water in 2015 (Samdal et al., 2020). Further analyses have now revealed that the relative concentrations of total MCs by LC–HRMS in cyanobacterial cells captured from filtered water samples collected from the lake during crayfish sampling in 2015 paralleled the ELISA results. Furthermore, LC–HRMS revealed the presence of an array of Dhb^7- and Mdha^7--containing [D-Asp^3]MC-variants in the water that is typical for mixed blooms of *Planktothrix* spp. in Lake Steinsfjorden (Miles et al., 2013a). The MC profile in the crayfish, on the other hand, only resembled the MC profile in the water in early summer, when the levels of *Planktothrix* were at their highest during the study period. Throughout the late summer, when *Planktothrix* and MC levels in the lakewater were relatively low, the levels of MCs in the crayfish not only remained high, but the MC profile in the stomachs of the animals changed dramatically to a suite of variants that had not been present in the water column at the sampling location (1–1.5 km from the crayfish harvesting area). This finding rules out one of the two potential explanations put forward in the study of Samdal et al. (2020), i.e. that the discrepancy between MCs in the water and crayfish could be due to slow depuration of the toxins from the crayfish. The most likely explanation for the combined ELISA, LC–HRMS and PCR results presented here and by Samdal et al. (2020), is that the MCs in the crayfish late in the summers of 2015 and 2016 originated from a non-planktonic source, possibly an MC-producing summer-active benthic cyanobacterium, a contaminated prey species, or a combination of both.

The prominent presence of the novel MCs such as MC-LHnv (**25**), MC-LNao (**22**), and MC-LCit (**16**) in the crayfish in late summer raises the possibility that MC-LR (**12**) can be metabolised on its Arg^4-side-chain in crayfish, or in the non-planktonic source of these MCs. If the metabolism in crayfish was the source of these analogues, then metabolism of D-Asp^3-variants [D-Asp^3]MC-RR (**3**) and [D-Asp^3,Dhb^7]MC-RR (**4**) could be expected to have occurred to produce the corresponding Dhb^7-and Mdha^7-variants of [D-Asp^3]MC-RHnv in May and June. However, neither these, nor the corresponding [D-Asp^3]MC-RCit variants, were detected in crayfish during the study period, suggesting that the Hnv, Cit, and Nao variants of MCs in the crayfish probably originate from the non-planktonic source.

Regardless of the origin of the novel MCs in the crayfish in the summer and autumn, there was no significant correlation between total MCs in the crayfish and the levels of cyanobacteria or MCs in the water in this study. Consequently, monitoring of cyanobacteria or MCs in the water column in Lake Steinsfjorden cannot be relied on as a guide to the levels of MCs in noble crayfish in this lake for the purposes of food safety assessment.

Credit author statement

Christopher O. Miles: Conceptualization, Investigation, Formal analysis, Visualization, Writing – Original Draft, Review & Editing. David A. Strand: Conceptualization, Field work, Investigation, Writing - Review & Editing. Johannes C. Rusch: Field work, Investigation, Formal analysis, Writing - Review & Editing. Andreas Ballot: Conceptualization, Investigation, Formal analysis, Writing - Review & Editing. Sigrid Haande: Conceptualization, Field work, Investigation, Writing - Review & Editing. Kjersti E. Løvberg: Formal analysis, Investigation. Trude Vrålstad: Conceptualization, Writing - Review & Editing, Funding acquisition, Project administration, Writing - Review & Editing. Ingunn A. Samdal: Conceptualization, Investigation, Data analysis, Visualization, Writing – Original Draft, Writing - Review & Editing, Resources.

Funding

This research was funded by The Research Council of Norway in the project: "TARGET – Targeted strategies for safeguarding the noble crayfish against alien and emerging threats" (grant 243907) and supported by National Research Council Canada and the Norwegian Veterinary Institute.

Declaration of competing interest

The authors declare that they have no known competing financial interests or personal relationships that could have appeared to influence the work reported in this paper.

Data availability

Data will be made available on request.

Acknowledgements

We thank the county governor of Buskerud (now Oslo & Viken) for a legal permit for catching crayfish for research purposes outside the legal crayfish fishing season. Noble crayfish were collected with the kind help of the Lake Steinsfjorden Fishery Association. We thank Vladyslava Hostyeva, NIVA, for assistance with the Adda-ELISA, and Elliott J. Wright for preparing the mixed CRM standards and dilution series.

Appendix A. Supplementary data

Supplementary data to this article can be found online at https://doi.org/10.1016/j.envres.2023.117623.

References

Armstrong, M.D., 1979. N^{δ}-acetylornithine and *S*-methylcysteine in blood plasma. Biochim. Biophys. Acta 587, 638–642. https://doi.org/10.1016/0304-4165(79)90015-1.

Artsdatabanken, 2021. Norsk Rødliste for Arter 2021. Available online: https://www.artsdatabanken.no/lister/rodlisteforarter/2021. (Accessed 14 April 2023).

Aune, T., Ramstad, H., Skulberg, O.M., Underdal, B., Yndestad, M., Østensvik, Ø., 1997. Cyanobakterier og edelkreps–toksinproduserende blågrønnalger i Steinsfjorden sommeren 1997; Norges veterinærhøgskole, Institutt for farmakologi, mikrobiologi og næringsmiddelhygiene and Norsk institutt for. vannforskning. Oslo, Norway.

Ballot, A., Swe, T., Mjelde, M., Cerasino, L., Hostyeva, V., Miles, C.O., 2020. Cylindrospermopsin- and deoxycylindrospermopsin-producing *Raphidiopsis raciborskii* and microcystin-producing *Microcystis* spp. in Meiktila Lake, Myanmar. Toxins 12, 232. https://doi.org/10.3390/toxins12040232.

Bouaïcha, N., Miles, C.O., Beach, D.G., Labidi, Z., Djabri, A., Benayache, N.Y., Nguyen-Quang, T., 2019. Structural diversity, characterization and toxicology of microcystins. Toxins 11, 714. https://doi.org/10.3390/toxins11120714.

Bownik, A., 2013. Effects of cyanobacterial toxins, microcystins on freshwater invertebrates. Pol. J. Nat. Sci. 28, 185–195.

Cantoral Uriza, A.E., Asencio, D.A., Aboal, M., 2017. Are we underestimating benthic cyanotoxins? Extensive sampling results from Spain. Toxins 9, 385. https://doi.org/10.3390/toxins9120385.

Flores, E., Arévalo, S., Burnat, M., 2019. Cyanophycin and arginine metabolism in cyanobacteria. Algal Res. 42, 101577 https://doi.org/10.1016/j.algal.2019.101577.

Foss, A., Miles, C.O., Samdal, I.A., Løvberg, K.E., Wilkins, A.L., Rise, F., Jaabæk, J.A.H., McGowan, P.C., Aubel, M.T., 2018. Analysis of free and metabolized microcystins in samples following a bird mortality event. Harmful Algae 80, 117–129. https://doi.org/10.1016/j.hal.2018.10.006.

Gaget, V., Humpage, A.R., Huang, Q., Monis, P., Brookes, J.D., 2017. Benthic cyanobacteria: a source of cylindrospermopsin and microcystin in Australian drinking water reservoirs. Water Res. 124, 454–464. https://doi.org/10.1016/j.watres.2017.07.073.

Gutierrez-Praena, D., Jos, A., Pichardo, S., Moreno, I.M., Camean, A.M., 2013. Presence and bioaccumulation of microcystins and cylindrospermopsin in food and the effectiveness of some cooking techniques at decreasing their concentrations: a review. Food Chem. Toxicol. 53, 139–152. https://doi.org/10.1016/j.fct.2012.10.062.

Halstvedt, C.B., Rohrlack, T., Andersen, T., Skulberg, O., Edvardsen, B., 2007. Seasonal dynamics and depth distribution of *Planktothrix* spp. in Lake Steinsfjorden (Norway) related to environmental factors. J. Plankton Res. 29, 471–482. https://doi.org/10.1093/plankt/fbm036.

Hao, G., Wang, D., Gu, J., Shen, Q., Gross, S.S., Wang, Y., 2009. Neutral loss of isocyanic acid in peptide CID spectra: a novel diagnostic marker for mass spectrometric

identification of protein citrullination. J. Am. Soc. Mass Spectrom. 20, 723–727. https://doi.org/10.1016/j.jasms.2008.12.012.
Hill, R.E., White, R.L., Smith, K.C., 1993. The identification of 5-hydroxy-L-norvaline in cultures of pyridoxine auxotrophs of *Escherichia coli* B. J. Nat. Prod. 56, 1246–1254. https://doi.org/10.1021/np50098a007.
Hollingdale, C., Thomas, K., Lewis, N., Békri, K., McCarron, P., Quilliam, M.A., 2015. Feasibility study on production of a matrix reference material for cyanobacterial toxins. Anal. Bioanal. Chem. 407, 5353–5363. https://doi.org/10.1007/s00216-015-8695-1.
IUCN, 2022. The IUCN red list of threatened species. version 2022-2. Available online: http://www.iucnredlist.org. (Accessed 14 April 2023).
Jiang, X., Smith, J.B., Abraham, E.C., 1996. Identification of a MS–MS fragment diagnostic for methionine sulfoxide. J. Mass Spectrom. 31, 1309–1310.
Johnsen, S.I., Strand, D., Rusch, J., Vrålstad, T., 2019. Nasjonal overvåking av edelkreps og spredning av signalkreps - presentasjon av overvåkingsdata og bestandsstatus - norsk intitutt for naturforskning Rapport 1590. Available online: https://brage.nina.no/nina-xmlui/handle/11250/2589548. .
Johnsen, S.I., Vrålstad, T., 2017. Edelkreps (*Astacus astacus*) - naturfaglig utredning og forslag til samordning av overvåkingsprogrammene for edelkreps og krepsepest. Available online: https://brage.nina.no/nina-xmlui/handle/11250/2446549.
Jones, M.R., Pinto, E., Torres, M.A., Dörr, F., Mazur-Marzec, H., Szubert, K., Tartaglione, L., Dell'Aversano, C., Miles, C.O., Beach, D.G., McCarron, P., Sivonen, K., Fewer, D.P., Jokela, J., Janssen, E.M.L., 2021. CyanoMetDB, a comprehensive public database of secondary metabolites from cyanobacteria. Water Res. 196, 117017 https://doi.org/10.1016/j.watres.2021.117017.
Kondo, F., Ikai, Y., Oka, H., Okumura, M., Ishikawa, N., Harada, K., Matsuura, K., Murata, H., Suzuki, M., 1992. Formation, characterization, and toxicity of the glutathione and cysteine conjugates of toxic heptapeptide microcystins. Chem. Res. Toxicol. 5, 591–596. https://doi.org/10.1021/tx00029a002.
Kurmayer, R., Christiansen, G., Gumpenberger, M., Fastner, J., 2005. Genetic identification of microcystin ecotypes in toxic cyanobacteria of the genus *Planktothrix*. Microbiology 151, 1525–1533. https://doi.org/10.1099/mic.0.27779-0.
Lirås, V., Lindberg, M., Nystrom, P., Annadotter, H., Lawton, L.A., Graf, B., 1998. Can ingested cyanobacteria be harmful to the signal crayfish (*Pacifastacus leniusculus*)? Freshw. Biol. 39, 233–242. https://doi.org/10.1046/j.1365-2427.1998.00278.x.
Mallia, V., Uhlig, S., Rafuse, C., Meija, J., Miles, C.O., 2019. Novel microcystins from *Planktothrix prolifica* NIVA-CYA 544 identified by LC–MS/MS, functional group derivatization and ^{15}N-labeling. Mar. Drugs 17, 643. https://doi.org/10.3390/md17110643.
Miles, C.O., 2017. Rapid and convenient oxidative release of thiol-conjugated forms of microcystins for chemical analysis. Chem. Res. Toxicol. 30, 1599–1608. https://doi.org/10.1021/acs.chemrestox.7b00121.
Miles, C.O., Melanson, J.E., Ballot, A., 2014. Sulfide oxidations for LC–MS analysis of methionine-containing microcystins in *Dolichospermum flos-aquae* NIVA-CYA 656. Environ. Sci. Technol. 48, 13307–13315. https://doi.org/10.1021/es5029102.
Miles, C.O., Sandvik, M., Haande, S., Nonga, H., Ballot, A., 2013a. LC–MS analysis with thiol derivatization to differentiate [Dhb^7]- from [Mdha^7]-microcystins: analysis of cyanobacterial blooms, *Planktothrix* cultures and European crayfish from Lake Steinsfjorden, Norway. Environ. Sci. Technol. 47, 4080–4087. https://doi.org/10.1021/es305202p.
Miles, C.O., Sandvik, M., Nonga, H.E., Rundberget, T., Wilkins, A.L., Rise, F., Ballot, A., 2013b. Identification of microcystins in a Lake Victoria cyanobacterial bloom using LC–MS with thiol derivatization. Toxicon 70, 21–31. https://doi.org/10.1016/j.toxicon.2013.03.016.
Miles, C.O., Stirling, D.J., 2018. Toxinmasslist COM v15b. Available online: https://doi.org/10.13140/RG.2.2.15794.50889. . (Accessed 11 October 2018).
Miles, C.O., Stirling, D.J., 2019. Toxin mass list COM v16.0 (microcystin and nodularin lists and mass calculators for mass spectrometry of microcystins, nodularins, saxitoxins and anatoxins). Available online: https://doi.org/10.13140/RG.2.2.12580.22402. . (Accessed 28 March 2023).
Mondal, S., Thompson, P.R., 2019. Protein arginine deiminases (PADs): biochemistry and chemical biology of protein citrullination. Accounts Chem. Res. 52, 818–832. https://doi.org/10.1021/acs.accounts.9b00024.
Papadimitriou, T., Kagalou, I., Stalikas, C., Pilidis, G., Leonardos, I.D., 2012. Assessment of microcystin distribution and biomagnification in tissues of aquatic food web compartments from a shallow lake and evaluation of potential risks to public health. Ecotoxicology 21, 1155–1166. https://doi.org/10.1007/s10646-012-0870-y.
Rohrlack, T., Edvardsen, B., Skulberg, R., Halstvedt, C.B., Utkilen, H.C., Ptacnik, R., Skulberg, O.M., 2008. Oligopeptide chemotypes of the toxic freshwater cyanobacterium *Planktothrix* can form sub-populations with dissimilar ecological traits. Limnol. Oceanogr. 53, 1279–1293. https://doi.org/10.4319/lo.2008.53.4.1279.
Samdal, I.A., Ballot, A., Løvberg, K.E., Miles, C.O., 2014. Multihapten approach leading to a sensitive ELISA with broad cross-reactivity to microcystins and nodularin. Environ. Sci. Technol. 48, 8035–8043. https://doi.org/10.1021/es5012675.
Samdal, I.A., Strand, D.A., Ballot, A., Rusch, J.C., Haande, S., Løvberg, K.L.E., Miles, C.O., Vrålstad, T., 2020. Microcystins in European noble crayfish *Astacus astacus* in Lake steinsfjorden, a *Planktothrix*-dominated lake. Toxins 12, 298. https://doi.org/10.3390/toxins12050298.
Skurdal, J., Garnas, E., Taugbol, T., 2002. Management strategies, yield and population development of the noble crayfish *Astacus astacus* in Lake Steinsfjorden. Bull. Fr. Peche Piscic. https://doi.org/10.1051/kmae:2002072, 845−860.
Tricarico, E., Bertocchi, S., Brusconi, S., Casalone, E., Gherardi, F., Giorgi, G., Mastromei, G., Parisi, G., 2008. Depuration of microcystin-LR from the red swamp crayfish *Procambarus clarkii* with assessment of its food quality. Aquaculture 285, 90–95. https://doi.org/10.1016/j.aquaculture.2008.08.003.
Yan, J., Lipka, A.E., Schmelz, E.A., Buckler, E.S., Jander, G., 2014. Accumulation of 5-hydroxynorvaline in maize (*Zea mays*) leaves is induced by insect feeding and abiotic stress. J. Exp. Bot. 66, 593–602. https://doi.org/10.1093/jxb/eru385.
Yilmaz, M., Foss, A.J., Miles, C.O., Özen, M., Demir, N., Balcı, M., Beach, D.G., 2019. Comprehensive multi-technique approach reveals the high diversity of microcystins in field collections and an associated isolate of *Microcystis aeruginosa* from a Turkish lake. Toxicon 167, 87–100. https://doi.org/10.1016/j.toxicon.2019.06.006.